FEBS Letters 585 (2011) 1197–1202

journal homepage: www.FEBSLetters.org

NMR studies of the solution conformation of the sex peptide from *Drosophila melanogaster*

Kerstin Moehle [a], Annabelle Freund [a], Eric Kubli [b], John A. Robinson [a,*]

[a] Chemistry Department, University of Zurich, Winterthurerstrasse 190, 8057 Zurich, Switzerland
[b] Institute of Molecular Life Sciences, University of Zurich, Winterthurerstrasse 190, 8057 Zurich, Switzerland

ARTICLE INFO

Article history:
Received 14 January 2011
Revised 11 March 2011
Accepted 17 March 2011
Available online 23 March 2011

Edited by Christian Griesinger

Keywords:
Peptide
Secondary structure
Conformation
Sex peptide
NMR spectroscopy
Fruit fly
Drosophila

ABSTRACT

The insect sex peptide (SP) elicits a variety of biological responses upon transfer to the mated female. SP contains 36 amino acids, including a tryptophan-rich N-terminal region, a central region containing five hydroxyproline (Hyp) residues, and a C-terminal region enclosed by a disulfide bridge. The solution structure of SP, studied here using NMR spectroscopy, includes a motif WPWN that adopts a type I β-turn in the N-terminal Trp-rich region. This turn region is connected to the central Hyp-rich region, which adopts extended and/or PPII-like conformations. The C-terminal disulfide-bonded loop populates helical turns or nascent helical structure. Overall, the results reveal a rather flexible peptide that lacks a compact folded structure in solution.

1. Introduction

The peptide hormone known as sex peptide (SP) is produced in seminal fluid of the male fruit fly (*Drosophila melanogaster*), where it elicits a variety of responses upon transfer to the mated female. These include changes in female sexual behaviour (oviposition and receptivity), as well as food intake, egg production, Juvenile hormone (JH) synthesis, ovulation, and antimicrobial peptide synthesis [1,2]. Thus SP probably interacts with several different receptors. One of these receptors was shown recently to be a G-protein coupled receptor (GPCR) called the sex peptide receptor (SPR) or CG16752 [3], which is located in various parts of the insect neuronal and ovarian systems [4]. The interaction of SP with SPR was shown to be responsible for eliciting oviposition and reduction of receptivity [3]. A different insect GPCR called Methuselah, which is associated with longevity, is also activated by binding to SP but the physiological relevance of this interaction remains unclear [5]. In addition, SP has been shown to elicit a systemic and epithelial innate immune response involving the production of the insect antimicrobial peptide drosocin, suggesting that SP may interact with pattern recognition receptors in the innate immune system of the insect [6,7].

The secreted mature SP contains 36 amino acids, including a tryptophan-rich N-terminal segment, a central region containing five hydroxyproline (Hyp) residues, and a C-terminal region enclosed by a disulfide bridge (Fig. 1) [8,9]. The Hyp was shown to be (2*S*,4*R*)-4-hydroxyproline by comparison to a synthetic standard [9], and is consistent with the ability of all known prolyl-4-hydroxylases, including that from *D. melanogaster*, to incorporate the hydroxyl group in the *R*-configuration. The biological functions of SP appear to be mediated by specific parts of the peptide [6]. Thus SPR interacts with the C-terminal disulfide-bridged loop, as this is the region needed for binding of SP to the nervous system and genital tract of females, and the same region is also essential for eliciting oviposition and reduction of receptivity [10,11]. The amino-terminal portion of SP is essential for inducing the synthesis of JH and for binding to sperm [12], whereas the Hyp-rich central region is an elicitor of the innate immune response, perhaps acting by chemical mimicry of sugar components of the bacterial cell wall [6].

In this work, we investigate the conformational behavior of SP using NMR spectroscopy in water and water/trifluoroethanol (TFE) solution. Information about the structure of SP in solution is of interest in understanding how this peptide hormone might

* Corresponding author.
E-mail address: robinson@oci.uzh.ch (J.A. Robinson).

0014-5793/$36.00
doi:10.1016/j.febslet.2011.03.040

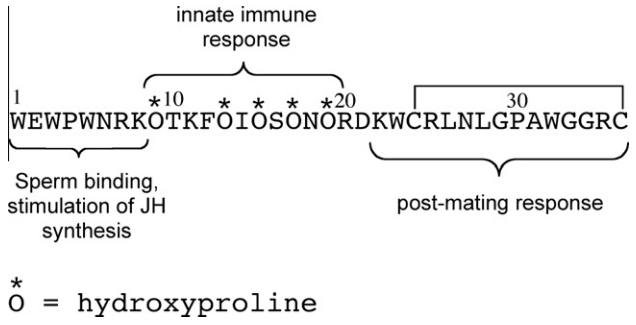

Fig. 1. The sequence of SP. The normal single letter amino acid code is used, except for O* = *trans*-L-4-hydroxyproline. The regions associated with specific biological responses are also shown (JH = juvenile hormone).

interact with various different receptors in the insect nervous, ovarian and immune systems.

2. Material and methods

2.1. Peptide synthesis

SP was synthesized on an *Applied Biosystems* peptide synthesizer ABI 433A using standard Fmoc chemistry. The following side-chain protected amino acids were used for the synthesis: Fmoc-Ala-OH, Fmoc-Asn(Trt)-OH, Fmoc-Asp(tBu)-OH, Fmoc-Arg(Pbf)-OH, Fmoc-Cys(Trt)-OH, Fmoc-Glu(tBu)-OH, Fmoc-Gly-OH, Fmoc-Ile-OH, Fmoc-Leu-OH, Fmoc-Lys(Boc)-OH, Fmoc-Phe-OH, Fmoc-Hyp(tBu)-OH, Fmoc-Ser(tBu)-OH, Fmoc-Thr(tBu)-OH and Fmoc-Trp(Boc)-OH. Fmoc deprotection was performed using 20% piperidine in NMP. Coupling reactions were carried out using HBTU/HOBt (4 equiv) in DMF and DIEA (8 equiv) in NMP. The activated amino acids (4 equiv) were coupled for 30 min. Capping was performed at the end of each cycle using a solution of HOBt (0.015 M), Ac_2O (0.5 M) and DIEA (0.125 M) in NMP.

SP was assembled on 2-chlorotrityl resin preloaded with Fmoc-Cys(Trt)-OH (0.24 mmol, 0.4 mmol/g, 600 mg). At the end of the synthesis, the peptide was cleaved from the resin and deprotected in a solution of TFA/EDT/H_2O/TIS 92.5:2.5:2.5:2.5 (30 mL) with shaking for 4 h at room temperature. After concentration in vacuo, the crude peptide was precipitated by addition of cold Et_2O (10 mL), collected by centrifugation, washed twice with Et_2O and dried in vacuo. The crude product was dissolved in H_2O+1% TFA (15 mL) and the solution was stored overnight at 4 °C to complete the deprotection of tryptophan residues. The crude peptide was then directly purified by reverse-phase HPLC on a preparative C_{18} column (Zorbax Eclipse XDB-C18; 21 × 250 mm, 10 μm, 80 Å) using a gradient of 15–50% acetonitrile in water (+0.1% TFA) over 16 min. Reduced SP was obtained as a white powder (90 mg, 20.4 μmol, 17% yield). HPLC purity >98% on an analytical C_{18} column (Zorbax Eclipse XDB-C18; 4.6 × 250 mm, 5 μm, 80 Å) using a gradient of 5–50% acetonitrile in water (+0.1% TFA) over 16 min. R_t = 15.7 min. MALDI-TOF: (m/z) 4429.1 $[M+H]^+$ (±0.1%; $M_{calc.}$ = 4428.1).

The reduced peptide (4.5 μmol, 20 mg) was dissolved in a solution of ammonium acetate buffer (20 ml, 50 mM, pH 8), and stirred in air at room temperature for 40 h. The peptide was purified by reverse-phase HPLC on a semi-preparative C_{18} column (Zorbax Eclipse XDB-C18; 10 × 250 mm, 10 μm, 80 Å) using a gradient of 5–50% acetonitrile in water (+0.1% TFA) over 16 min. After lyophilization SP was obtained as a white solid (12 mg) in 60% yield. The product was ⩾98% pure by reverse-phase HPLC (analytical C_{18} column, Zorbax Eclipse XDB-C18; 4.6 × 250 mm, 5 μm, 80 Å, using a gradient of 5–50% acetonitrile in water (+0.1% TFA) over 16 min). R_t = 15.7 min. MALDI-TOF: (m/z) 4427.3 $[M+H]^+$ (±0.1%; $M_{calc.}$ = 4426.3).

Synthetic SP was assayed for oviposition and receptivity according to standard procedures [8], and was found to show full activity.

2.2. NMR spectroscopy and structure calculations

^1H NMR measurements were performed in H_2O/D_2O (9:1) or pure D_2O, pH 5.0; or in a mixture (1:1) of trifluoroethanol (TFE-d_3) and H_2O/D_2O (9:1), pH 5.0. Spectra were acquired on either a Bruker AV-600 or AV-700 spectrometer at 300 K. Data were processed using TOPSPIN 2.1 (Bruker) or XEASY [13]. 1D ^1H NMR spectra were also recorded at various temperatures (279, 286, 293, 307 and 314 K), pH values (4, 6 and 7) and SP concentrations (0.07, 0.13, 0.27 and 0.68 mM). Water suppression was performed by presaturation. Spectral assignments were made for water and TFE/water solutions using 2D DQF-COSY, TOCSY and NOESY spectra. $^3J_{HN\alpha}$ coupling constants were determined from 1D spectra or from 2D NOESY spectra by inverse Fourier transformation of in-phase multiplets [14].

[^{15}N, ^1H]- and [^{13}C,^1H]-HSQC spectra at natural abundance were recorded using 3 mM peptide samples in H_2O/D_2O 9:1, and in pure D_2O. Acquisition data were sampled as 1024 × 128 or 1024 × 200 complex points in t2 and t1, for the ^{15}N and ^{13}C correlation spectra, respectively. The 2D data matrices were multiplied by a square-sine-bell window function and zero filled to 2 × 1 k or 2 × 2 k points prior to Fourier transformation. Baseline correction was applied in both dimensions. Spectra were referenced in the direct dimension to the water signal and in the ^{15}N dimension using the ^{15}N to ^1H frequency ratio of 0.101329118, while carbon referencing was directly performed on the internal TSP standard (0 ppm).

Distance restraints were obtained from NOESY spectra with a mixing time of 200 ms. Spectra were typically collected with 1024 × 256 complex data points zero-filled prior to Fourier transformation to 2048 × 1024, and transformed with a cosine-bell weighting function. The structure calculations were performed by restrained molecular dynamics in torsion angle space using DYANA [15], using only the NOE-derived distance restraints. Starting from 100 randomized conformations a bundle of 20 conformations were selected, which encur the lowest DYANA target energy function. The program MOLMOL [16] was used for structure analysis and visualization of the molecular models. The structures have been deposited in the Protein Data Bank (PDB code 2LAQ).

Time-averaged restrained MD simulations were carried out using GROMACS v4.5.3 [17] with the AMBER99 force field in explicit solvent and periodic boundary conditions. The initial structure was selected from the calculated NMR structures. The peptide was placed in a rhombic dodecahedral unit cell with a minimum distance of 1.2 nm to the box edge. TIP3P water molecules and ions to counterbalance the peptide charge were added yielding a final system of 16338 water molecules and 5 Cl^- ions. Steepest decent minimization was performed. Electrostatics were treated with particle-mesh Ewald (PME) using a short range cut-off, and a cut-off for van der Waals forces of 1.4 nm. After 20 ps equilibration with position restraints on peptide heavy atoms, a 10 ns simulation with time-averaged NOE distance restraints (Table S3) was performed. In all simulations the temperature was maintained close to 300 K by weak coupling to an external bath with a coupling constant of 0.1 ps. The LINCS algorithm was used to constrain all bond lengths.

3. Results and discussion

A series of 1D ^1H NMR spectra at varying pH and peptide concentrations revealed only marginal changes in shape and

dispersion of NMR signals, suggesting that the peptide does not aggregate significantly under these conditions. ^{1}H NMR spectra in water and in TFE/water (1:1) mixtures revealed two species in a ratio of approximately 1:3 and 1:5, respectively, which interconvert slowly on the NMR timescale, representing *cis-trans* isomers at the Trp^{3}-Pro^{4} peptide bond. The major species was the *trans*-isomer at all Xaa-Pro and Xaa-Hyp bonds, as indicated by Hα-Hδ NOE connectivities between the corresponding residues. When NMR spectra were recorded in D_2O, all the peptide NH groups exchanged rapidly (within the time of the NMR measurement), indicating the absence of stable intramolecular hydrogen bonded structures.

Chemical shifts. ^{1}H and ^{13}C chemical shift deviations (CSDs) from random coil values ($\Delta\delta = \delta^{observed} - \delta^{random}$) were examined for indications of regular secondary structure (Fig. 2) [18]. The patterns expected are positive values for $\Delta\delta_{H\alpha}$ and $\Delta\delta_{C\beta}$ and negative values for $\Delta\delta_{C\alpha}$ in β-strands, whereas values of opposite sign are

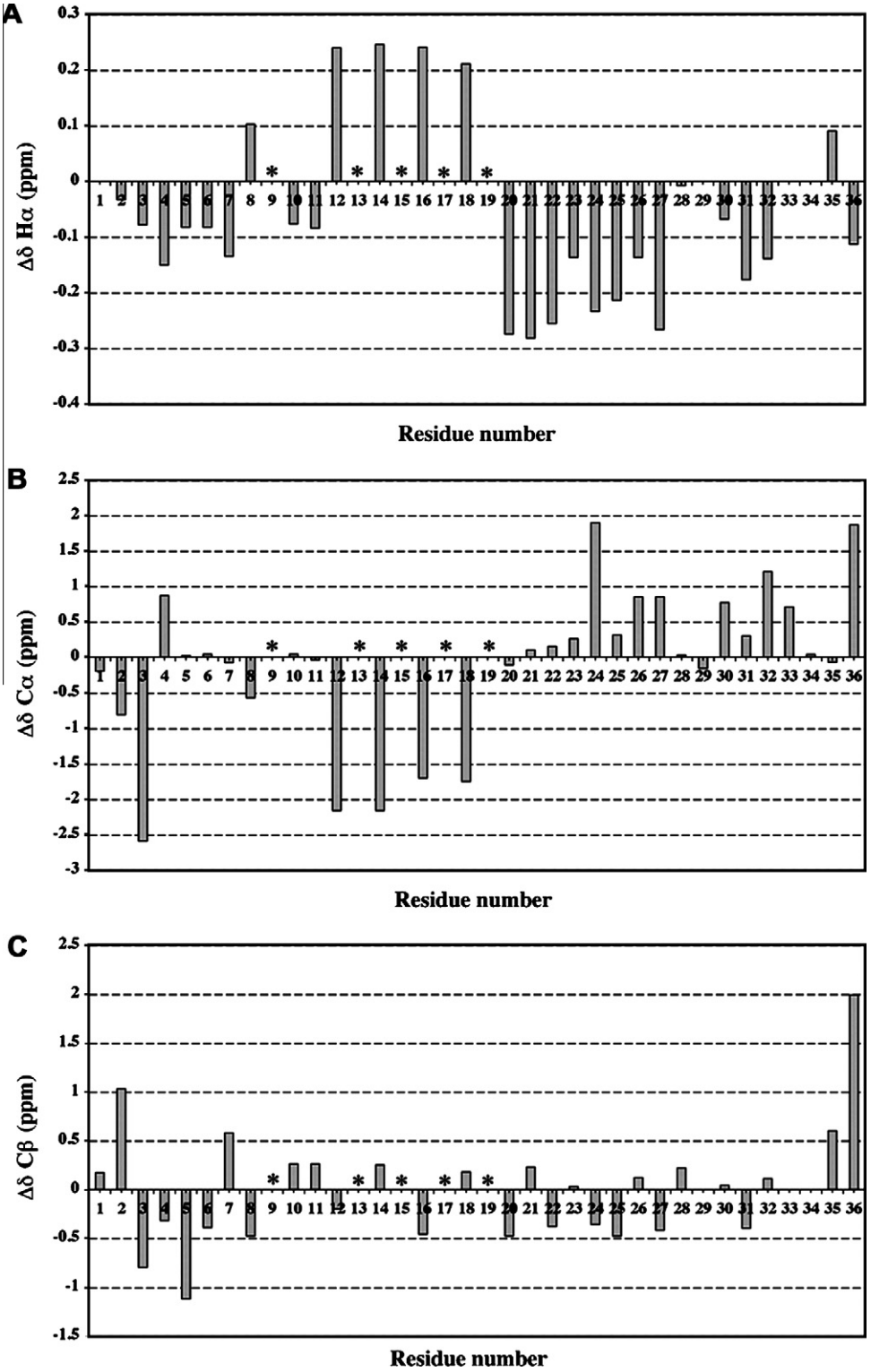

Fig. 2. ^{1}H and ^{13}C Chemical shift deviations (CSDs) from random coil values for residues 1–36 in SP ($\Delta\delta = \delta^{observed} - \delta^{random}$) for ^{1}Hα (A), ^{13}Cα (B) and ^{13}Cβ (C) resonances in water solution. The asterik shows the positions of hydroxyproline (Hyp) in the sequence. Values for Gly Hα are not included.

expected for α-helices [19]. The CSDs in the N-terminal Trp-rich region should be interpreted with caution, since they may be influenced by aromatic ring current as well as conformational effects [20], although analyses of NOEs provide evidence for a β-turn at the $Trp^3Pro^4Trp^5Asn^6$ motif (see below). In the central Hyp-rich region (the CSDs of Hyp have not been documented), the $\Delta\delta_{H\alpha}$ and $\Delta\delta_{C\alpha}$ values for non-Hyp residues clearly suggest that β-structure is favored (Fig. 2). The numerous Hyp residues, however, may have a special effect on the conformation of the peptide backbone in the central region. For example, the role of Hyp in stabilizing the triple helix in collagen is well known [21]. Also, proline residues are generally restricted to two narrow regions of dihedral space: the α-helical region at $(\phi,\psi) = (-61°,-35°)$ and the β-region at $(-65°, +150°)$ [22,23]. The extended conformation – the so-called left-handed polyproline II helical conformation (PPII) – is the dominant fold in pure polyproline peptides. The PPII conformation is an extended helical structure, with three residues per turn, which does not form intramolecular backbone hydrogen bonds [23]. While the PPII helix has a preference for proline residues, it is also found with other amino acids [23]. Furthermore, proline restricts the preceding residue to the β-region of dihedral (ϕ,ψ) space [22]. The CSDs observed for each amino acid preceding a Hyp residue are consistent with β- and/or PPII conformations. In the C-terminal region from Arg^{20}-Asn^{27}, the negative $\Delta\delta_{H\alpha}$, positive $\Delta\delta_{C\alpha}$, and negative $\Delta\delta_{C\beta}$ values provide support here for nascent helical secondary structure (Fig. 2). From Cys^{24} this includes several residues that form part of the disulfide-bridged loop. From Leu^{28} to the C-terminus this trend into negative CSDs is less apparent, suggesting that nascent helical structure does not extend into the second half of the disulfide-bridged loop. Interestingly, at the end of the helical section (Arg^{20}-Asn^{27}) the motif $Gly^{29}Pro^{30}Ala^{31}$ possesses a high propensity for β-turn formation. Indeed, NOEs are observed that support the occurrence of a nascent turn in this region of the SP backbone (see below).

All measured chemical shifts, including HA, CA, CB, HN and N (see Supplementary data), were also analyzed using TALOS+, a program that exploits the large database of protein NMR data to establish accurate relations between chemical shifts and backbone torsion angles ϕ and ψ [24]. Using these data, TALOS+ predicts with a "good" score (RCI-derived order parameter S^2 from 0.69 to 0.77) that all non-Hyp residues from Phe^{12}-Asn^{18} will occupy the β-region, and all residues from Trp^{23}-Leu^{28} the α-region of $\phi\psi$ space.

Coupling constants. Backbone $^3J_{HN\alpha}$ coupling constants $\leqslant$5 Hz are typical for residues in α-helices and >7 Hz for residues in regular β-structure [25]. However, most of the $^3J_{HN\alpha}$ values for SP in water are in the range 6–7 Hz (Fig. 3), which is consistent with a relatively flexible backbone and/or with PPII conformations. However, a series of lower $^3J_{HN\alpha}$ values are seen in the region Arg^{20}-Asn^{27} in water/TFE, adding further support for nascent helical structures in this region.

Nuclear overhauser effects. 2D-NOESY spectra revealed few long range NOEs (see below), suggesting that SP does not adopt a compact folded structure under the conditions tested (Fig. 3). Average solution structures for SP were calculated with DYANA using NOE-

Table 1
Experimental distance restraints and statistics for the final 20 NMR structures calculated for SP in water and TFE/water.

	Water	TFE/water
Number of NOE upper-distance limits	266	360
Intraresidue	101	127
Sequential	138	182
Medium- and long-range	27	51
Residual target function value (Å^2)	2.43 ± 0.40	1.49 ± 0.11
Residual NOE violations		
Number >0.2 Å	32	15
Maximum (Å)	0.5	0.44
Mean rmsd values (Å)		
Between Glu^2 and Lys^8		
Backbone atoms	2.05 ± 0.46	1.62 ± 0.54
All heavy atoms	4.62 ± 0.79	3.55 ± 0.97
Between Phe^{12} and Asn^{18}		
Backbone atoms	1.96 ± 0.57	2.10 ± 0.59
All heavy atoms	3.51 ± 0.81	3.62 ± 0.84
Between Lys^{22} and Cys^{36}		
Backbone atoms	2.90 ± 1.31	1.97 ± 0.57
All heavy atoms	4.44 ± 1.61	3.10 ± 0.78

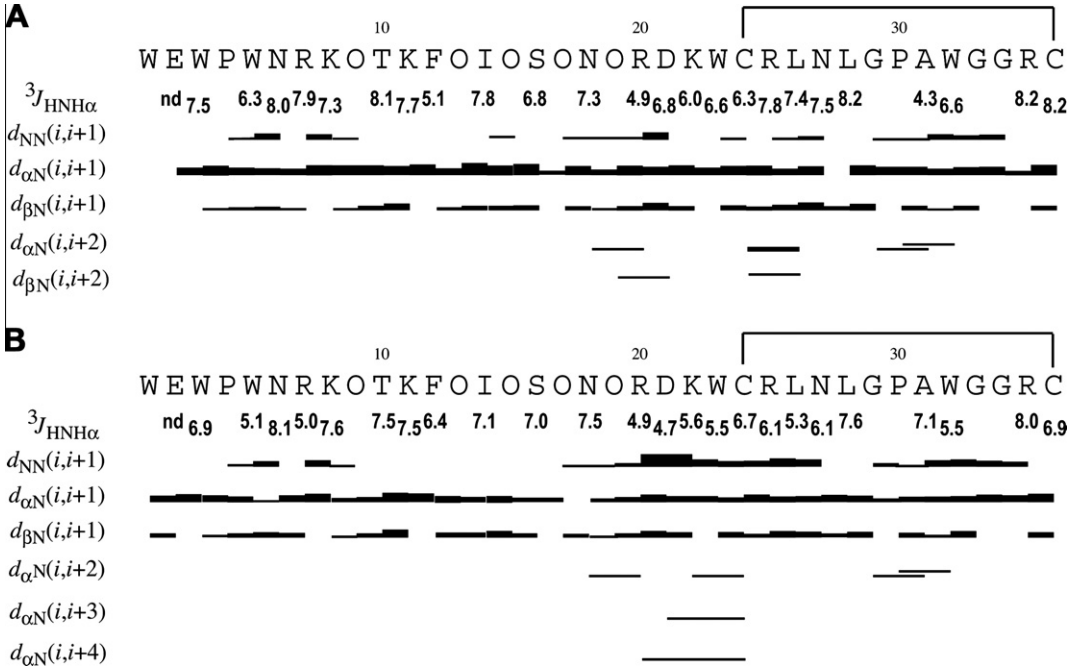

Fig. 3. NOEs and $^3J_{HN\alpha}$ values observed for SP in (A) water and (B) water/TFE (1:1) solution. The letter "O" indicates hydroxyproline. NOEs shown to peptide NH groups are to the $CH_2(\delta)$ for P and O residues.

derived distance restraints. Rather high mean rmsd values are obtained after global backbone superimposition of the final 20 structures. The observed NOEs, however, provide evidence for ordered secondary structure, or nascent structure, only in distinct regions of SP, which is supported also by analyses of CSDs and coupling constants (see above). The three regions of interest are the N-terminal Trp-rich sequence (Glu^2-Lys^8), the Hyp-rich central region (Phe^{12}-Asn^{18}), and the disulfide-bonded loop region (Lys^{22}-Cys^{36}). Upon superimposition of these individual regions in the final 20 structures, lower backbone rmsd values are obtained (Table 1). In addition, time-averaged NOE-derived distance restraints were applied in MD simulations in order to take account of flexibility in the SP backbone (see Supplementary data, Fig. S2).

In the N-terminal Trp-rich region of SP in TFE/water, sequential as well as multiple medium range NOEs (between Trp^3 and Trp^5/Asn^6 – see Supplementary data for a full list of NOE distance restraints) provide strong evidence for a well-defined type I β-turn in the WPWN motif. This turn is highly populated in the NMR structures calculated using DYANA (Fig. 4). This turn occurs in the *trans*-Trp^3-Pro^4 rotamer, and is characterized by the Trp^5 side chain stacking against the pyrrolidine ring of Pro^4 (Fig. 4B and C) and the side-chain of Trp^3. A much stronger Pro^4 Hα to Trp^5 HN NOE than actually observed would be expected if a type II turn were formed. Evidence for a type I turn is the upfield shifted Hα resonance for Pro^4 and downfield shifted of Hα in Trp^5 (Fig. 2), a combination that is typical for position 2/3 of only the type I turn [26]. On the other hand, for SP dissolved in water only two weak medium range NOEs are seen between Trp^3 and Trp^5. This suggests that a nascent rather than a stable turn is populated in this region in pure water. During the course of 10 ns time-averaged distance-restrained MD simulations (TAMD) in explicit water solvent, the Pro^4-Trp^5 remained in a type I turn (Fig. S2).

In the hydroxyproline-rich central region (Hyp^9-Hyp^{19}), only intra-residue and sequential NOEs are observed in both solvents. This

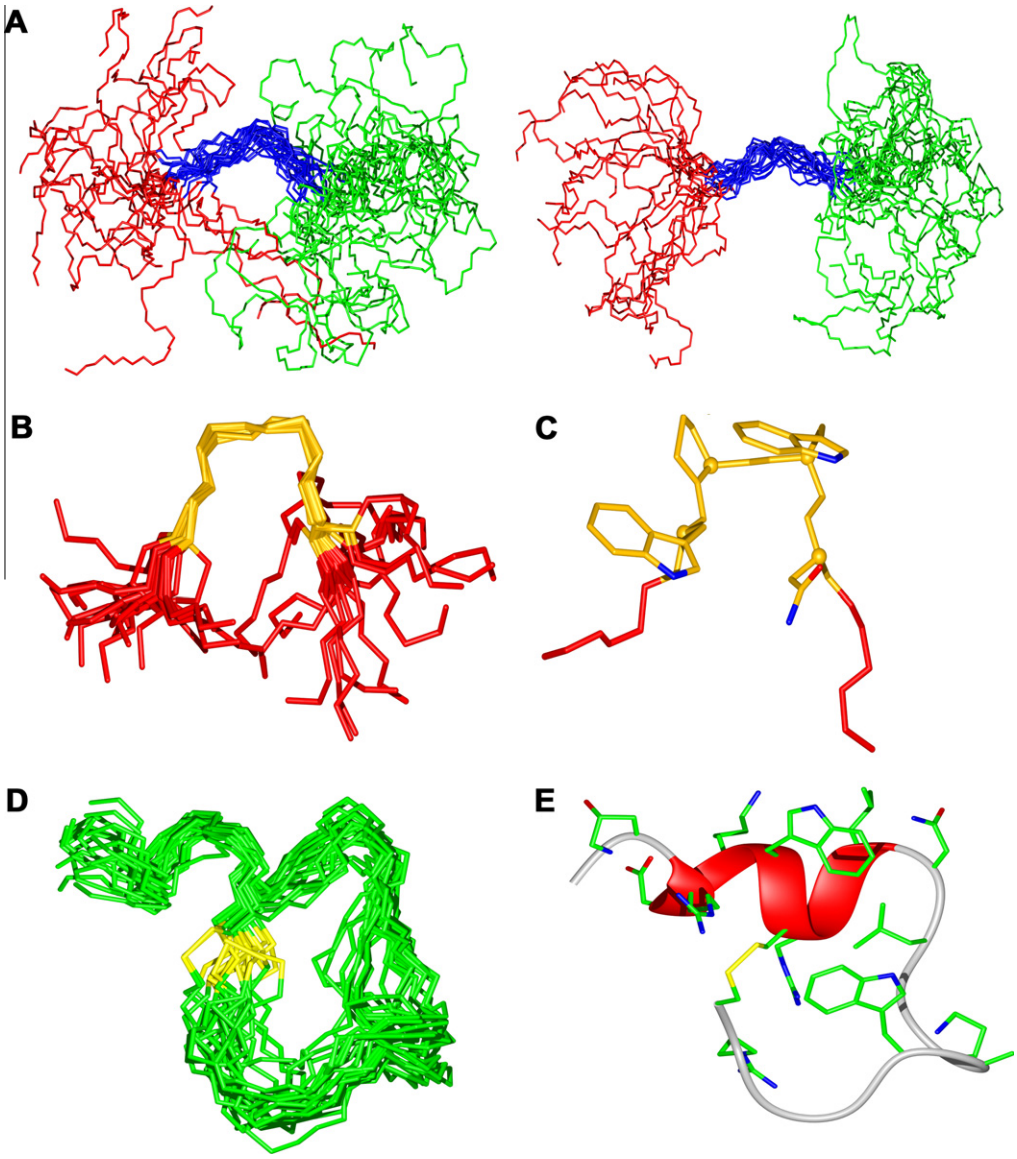

Fig. 4. (A) Backbone representation and superposition of the 20 DYANA NMR structures of SP using the backbone heavy atoms of Phe^{12} to Asn^{18} (in blue), observed in TFE/water (*left*) and water (*right*) (the N-terminal region between Trp^1 and Lys^{11} is shown in red, the C-terminal region between Hyp^{19} and Cys^{36} in green). (B) The Trp-rich N-terminal residues 1–8 in TFE/water superimposed (using the backbone heavy atoms) between Trp^3 and Asn^6 (in orange), showing the type I β-turn at WPWN. (C) Representative side chain orientation in the turn region between 3 and 6. (D) Backbone representation and superposition of SP in TFE/water between Hyp^{19} and Cys^{36} (disulfide bond in yellow). (E) Ribbon representation of one solution structure of the region Hyp^{19}-Cys^{36} showing the nascent helical element. The side chains of Trp^{23}, Leu^{26}, Leu^{28} and Trp^{32} are arranged in a hydrophobic patch.

and the observation of strong Hα(i)-Hδ(i + 1) and weak or absent HN(i)-Hδ(i + 1) NOEs, for each Xaa-Hyp pair, are consistent with extended and/or PPII conformations in this region. The same conclusion was also suggested from the CSD data, discussed above. It seems that this region may be extended and semi-rigid, as seen in the NMR structures shown in Fig. 4. The TAMD simulations support the high propensity of PPII conformations in this region, although turn conformations were also observed at Ser^{16}-Hyp^{17}, and Hyp^{19}-Arg^{20} (see Supplementary data).

In the region of the disulfide-bonded loop (Arg^{20}-Cys^{36}), a series of sequential HN-HN as well as medium range Hα(i)-NH(i + 2) and Hα(i)-NH(i + 3) NOEs are seen from Arg^{20} to Asn^{27}, particularly in water/TFE mixture. These NOEs are characteristic of α-helical conformations, or a nascent helix (in water) in this region, as suggested also by the CSD data discussed above. However, the TAMD simulations (Fig. S2) suggest more flexibility may be present in this region. A reversal of the peptide chain direction is needed for disulfide ring closure at the C-terminus, which is achieved by a turn conformation at Pro^{30}-Ala^{31}. A strong HN-HN NOE between Trp^{32}-Ala^{31}, a Hα–HN NOE between Trp^{32}-Pro^{30}, as well as the upfield shifted HN of Trp^{32} also support the occurrence here of turn-like structures. A type-I β-turn conformation at Pro^{30}-Ala^{31} is also stably maintained in the TAMD trajectory (Fig. S2), in agreement with the NMR data. Furthermore, long range NOEs between the side chains of Leu^{26}-Trp^{23}, and between Trp^{23}, Leu^{28} and Trp^{32} indicate that these amino acid side chains are clustered into a hydrophobic patch on the same side of the macrocycle (Fig. 4). Consistent with this clustering is the upfield shift of the Asn^{27} side chain protons, which in DYANA structures come into close contact to the Trp^{23} aromatic side chain. However, no evidence of regular secondary structure was observed in the final C-terminal segment between Trp^{32} and Cys^{36}.

The overall picture to emerge from these studies is of a flexible peptide that lacks a compact folded structure, but which nevertheless possesses elements of nascent secondary structure in distinct regions, in aqueous solution. This nascent structure becomes more pronounced in water/TFE mixtures. The N-terminal Trp-rich region contains a motif WPWN that forms type I β-turns. This turn region is connected to a central Hyp-rich region, which populates an extended and/or PPII-like conformation. Finally, towards the C-terminus and the disulfide-bonded loop, a region of nascent helical and another β-turn is found. These distinct regions of nascent secondary structure may be important for recognition of SP by its various cellular receptors.

Acknowledgements

This work was supported by the University of Zurich. Professor Oliver Zerbe is thanked for help with measurement of heteronuclear NMR spectra.

Appendix A. Supplementary data

Supplementary data associated with this article can be found, in the online version, at doi:10.1016/j.febslet.2011.03.040.

References

[1] Kubli, E. (2008) Sexual behaviour: a receptor for sex control in Drosophila females. Curr. Biol. 18, R210–R212.
[2] Kubli, E. (2010) Sexual behavior: dietary food switch induced by sex. Curr. Biol. 20, R474–R476.
[3] Yapici, N., Kim, Y.-J., Ribeiro, C. and Dickson, B.J. (2007) A receptor that mediated the post-mating switch in Drosophila reproductive behaviour. Nature 451, 33–37.
[4] Häsemeyer, M., Yapici, N., Heberlein, U. and Dickson, B.J. (2009) Sensory neurons in the Drosophila female reproductive tract regulate female reproductive behavior. Neuron 61, 511–518.
[5] Ja, W.W., Carvalho, G.B., Madrigal, M., Roberts, R.W. and Benzer, S. (2009) The Drosophila G protein-coupled receptor methuselah exhibits a promiscuous response to peptides. Protein Sci. 18, 2203–2208.
[6] Domanitskaya, E.V., Liu, H.F., Chen, S.J. and Kubli, E. (2007) The hydroxyproline motif of male sex peptide elicits the innate immune response in Drosophila females. FEBS J. 274, 5659–5668.
[7] Peng, J., Zipperlen, P. and Kubli, E. (2005) Drosophila sex-peptide stimulates female innate immune system after mating via the Toll and Imd pathways. Curr. Biol. 15, 1690–1694.
[8] Chen, P.S., Stumm-Zollinger, E., Aigaki, T., Balmer, J., Bienz, M. and Böhlen, P. (1988) A male accessory gland peptide that regulates reproductive behavior of female *D. melanogaster*. Cell 54, 291–298.
[9] Schmidt, T., Choffat, Y., Klauser, S. and Kubli, E. (1993) The *Drosophila melanogaster* sex-peptide: a molecular analysis of structure-function relationships. J. Insect Physiol. 39, 361–368.
[10] Ding, Z., Haussmann, I., Ottiger, M. and Kubli, E. (2003) Sex-peptides bind to two molecularly different targets in *Drosophila melanogaster* females. J. Neurobiol. 55, 372–384.
[11] Kubli, E. (2003) Sex-peptides: seminal peptides of the Drosophila male. Cell Mol. Life Sci. 60, 1689–1704.
[12] Peng, J., Chen, S., B¸sser, S., Liu, H., Honegger, T. and Kubli, E. (2005) Gradual release of sperm bound sex-peptide controls female postmating behavior in Drosophila. Curr. Biol. 15, 207–213.
[13] Bartels, C., Xia, T.-h., Billeter, M., Güntert, P. and Wüthrich, K. (1995) The program XEASY for computer-supported NMR spectral analysis of biological macromolecules. J. Biomol. NMR 6, 1–10.
[14] Szyperski, T., Güntert, P., Otting, G. and Wüthrich, K. (1992) Determination of scalar coupling constants by inverse Fourier transformation of in-phase multiplets. J. Mag. Res. 99, 552–560.
[15] Guntert, P., Mumenthaler, C. and Wuthrich, K. (1997) Torsion angle dynamics for NMR structure calculation with the new program DYANA. J. Mol. Biol. 273, 283–298.
[16] Koradi, R., Billeter, M. and Wuthrich, K. (1996) MOLMOL: a program for display and analysis of macromolecular structures. J. Mol. Graph. 14, 51–55.
[17] Hess, B., Kutzner, C., van der Spoel, D. and Lindahl, E. (2008) GROMACS 4: algorithms for highly efficient, load-balanced, and scalable molecular simulation. J. Chem. Theory Comp. 4, 435–447.
[18] Wishart, D.S., Bigam, C.G., Holm, A., Hodges, R.S. and Sykes, B.D. (1995) 1H, 13C and 15N random coil NMR chemical shifts of the common amino acids. I. Investigations of nearest-neighbor effects. J. Biomol. NMR 5, 67–81.
[19] Mulder, F.A.A. and Filatov, M. (2010) NMR chemical shift data and ab initio shielding calculations: emerging tools for protein structure determination. Chem. Soc. Rev. 39, 578–590.
[20] Schwarzinger, S., Kroon, G.J.A., Foss, T.R., Chung, J., Wright, P.E. and Dyson, H.J. (2001) Sequence-dependent correction of random coil NMR chemical shifts. J. Am. Chem. Soc. 123, 2970–2978.
[21] Gorres, K.L. and Raines, R.T. (2010) Prolyl 4-hydroxylase. Crit. Rev. Biochem. Mol. Biol. 45, 106–124.
[22] Macarthur, M.W. and Thornton, J.M. (1991) Influence of proline residues on protein conformation. J. Mol. Biol. 218, 397–412.
[23] Adzhubei, A.A. and Sternberg, M.J.E. (1993) Left-handed polyproline-Ii helices commonly occur in globular-proteins. J. Mol. Biol. 229, 472–493.
[24] Shen, Y., Delaglio, F., Cornilescu, G. and Bax, A. (2009) TALOS+: a hybrid method for predicting protein backbone torsion angles from NMR chemical shifts. J. Biomol. NMR 44, 213–223.
[25] Wüthrich, K. (1986) NMR of Proteins and Nucleic Acids, John Wiley & Sons, New York.
[26] Ösapay, K. and Case, D.A. (1994) Analysis of proton chemical shifts in regular secondary structure or proteins. J. Biomol. NMR 4, 215–230.